Human land-use-driven reduction of forest volatiles cools global climate

Nadine Unger

Human conversion of forest ecosystems to agriculture is a major driver of global change. Conventionally, the impacts of the historical cropland expansion on Earth's radiation balance have been quantified through two opposing effects: the release of stored carbon to the atmosphere as CO_2 (warming) versus the increase in surface albedo (cooling)[1]. Changing forest cover has a third effect on the global radiation balance by altering emissions of biogenic volatile organic compounds (BVOCs) that control the loadings of multiple warming and cooling climate pollutants: tropospheric ozone (O_3), methane (CH_4) and aerosols. Although human land cover change has dominated BVOC emission variability over the past century[2-4], the net effect on global climate has not been quantified. Here, I show that the effects of the global cropland expansion between the 1850s and 2000s on BVOC emissions and atmospheric chemistry have imposed an additional net global radiative impact of -0.11 ± 0.17 W m^{-2} (cooling). This magnitude is comparable to that of the surface albedo and land carbon release effects. I conclude that atmospheric chemistry must be considered in climate impact assessments of anthropogenic land cover change and in forestry for climate protection strategies.

Human land cover change has altered an estimated 50% of Earth's land surface, mostly through conversion of forest ecosystems to agricultural uses[5]. The IPCC Fifth Assessment Report (AR5) provides global radiative forcing values for the opposing effects of land use on CO_2 and surface albedo that have similar magnitudes but opposite sign: $+0.17$–0.51 W m^{-2} (1850–2000) versus -0.15 ± 0.10 W m^{-2} (1750–2011)[1]. The sign of the global average surface temperature response to these forcings due to human land cover change remains controversial[6,7]. Thus, it is not known whether large-scale human deforestation has contributed to global warming or global cooling[8,9].

Forest ecosystems return to the atmosphere about 1% of the annual carbon uptake by the land biosphere in the form of chemically reactive BVOCs (ref. 10). The ecological and physiological roles of BVOCs are broad, ranging from abiotic and biotic stress functions to integrated components of carbon metabolism. In the present-day climate state, the dominant BVOCs emitted are isoprene (400–600 TgC yr^{-1}) and monoterpenes (30–130 TgC yr^{-1}; ref. 10). Tropical and temperate vegetation tends to emit isoprene whereas boreal vegetation tends to emit monoterpenes. New-generation global BVOC emission models suggest that the BVOC emissions were about 20–25% higher in the pre-industrial climate state and that the cropland expansion is the major driver of the decrease in emissions over the past century[2-4]. This high sensitivity to human deforestation arises because of the strong BVOC emission dependence on ecosystem type: broadleaf forests are strong emitters whereas crops and grasses are weak emitters or even non-emitting[10].

BVOC emissions undergo rapid oxidation in the atmosphere, generating the climate pollutants O_3 and biogenic secondary organic aerosol (SOA; ref. 11). The photochemical processing of BVOC emissions influences the oxidation capacity of the atmosphere, which affects the lifetime of CH_4 and the production of other secondary aerosols, sulphate and nitrate, whose formation rates depend on the availability of oxidants[12]. O_3 and CH_4 are powerful greenhouse gases that warm the atmosphere. Aerosol particles (organics, sulphate and nitrate) predominantly scatter solar radiation back to space and lead to global cooling. The extent to which the past changes in BVOC emissions have altered global radiative forcing is not clear-cut at the outset because the perturbation involves multiple warming and cooling climate pollutants.

Here, a global carbon–chemistry–climate model is employed to investigate the effects of the historical cropland expansion between the 1850s and 2000s on the BVOC emissions and climate pollutants. A baseline simulation representative of the chemical and meteorological background atmosphere in the 2000s is performed. Land cover and anthropogenic emissions are prescribed using harmonized gridded datasets that were developed for the IPCC AR5 assessment[5,13]. Between the 1850s and 2000s the global crop cover fraction of vegetated land area more than doubles (14–37%) at the expense of grass (11–6%), shrub (6–3%), savanna (8–5%), deciduous (13–10%) and tropical rainforest (12–10%) (Supplementary Fig. 1). A sensitivity experiment is performed in which the 2000s baseline simulation is forced with the 1850s land cover dataset. The difference between these simulations allows faithful isolation of the effects of the 1850s–2000s land cover change on BVOC emissions and the climate pollutants and is defined as the case LAND. The 1850s land forcing also affects the climate pollutants via non-BVOC pathways, including hydrological cycle impacts on oxidant and aerosol sources and sinks, underlying surface albedo effects on aerosol–radiation interactions, and surface deposition rates. Therefore, a second pair of simulations is performed identical to above (2000s baseline and the 2000s baseline forced with the 1850s land cover dataset) but with the BVOC emissions held fixed at climatological monthly varying values for the 2000s. The difference between this simulation pair is defined as the case LAND-fixbvoc. In this case, the climate pollutants respond only to the non-BVOC mechanisms of land cover change.

I follow the IPCC's reporting structure and adopt the historical global mean annual average radiative forcing metric, which is a powerful indicator of the equilibrium global average surface temperature response to the perturbation. The global model is used to compute the radiative forcings due to O_3, biogenic SOA,
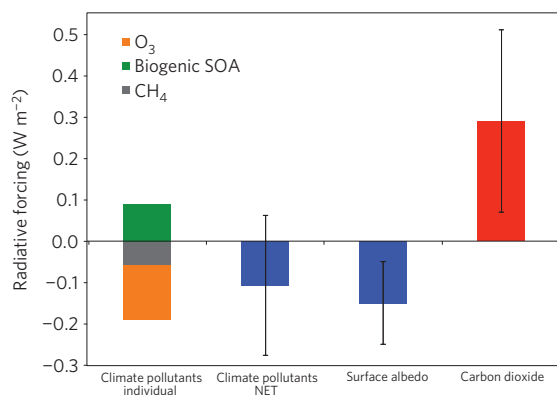
School of Forestry and Environmental Studies, Yale University, New Haven, Connecticut 06511, USA. e-mail: nadine.unger@yale.edu

Figure 1 | Global climate effects of historical cropland expansion (W m^{-2}). Climate pollutants are calculated in this study. Barred black lines indicate uncertainty range. Uncertainties for climate pollutants are assigned a best estimate of ±100% based on a factor of two uncertainty in BVOC emissions[10,24]. Values and uncertainty ranges for surface albedo and carbon dioxide release are from IPCC AR5 (ref. 1). The time period for each perturbation signal is 1850s–2000s, except for the surface albedo estimate, which refers to 1750–2011.

sulphate and nitrate for the LAND and LAND-fixbvoc cases. CH$_4$ radiative forcing is calculated off-line using the simulated changes in CH$_4$ chemical lifetime, which accounts for the indirect CH$_4$ effects on stratospheric water vapour and the longer-term O$_3$ response[14]. For two reasons this study does not consider aerosol–cloud interactions. First, the sign of the global radiation interaction between SOA and cloud in the present-day atmosphere is not robust across models, with published estimates ranging from +0.23 W m^{-2} to −0.77 W m^{-2} (refs 15,16). Second, there is evidence that isoprene, the dominant BVOC in the temperate and tropical biomes where the cropland expansion has occurred, acts to inhibit new particle nucleation[17].

In the 2000s baseline, the simulated global source strength of BVOC emissions is 607 TgC yr^{-1} (isoprene = 404 TgC yr^{-1}; monoterpene = 132 TgC yr^{-1}; other VOCs = 70 TgC yr^{-1}), which increases to 819 TgC yr^{-1} (isoprene = 539 TgC yr^{-1}; monoterpene = 184 TgC yr^{-1}; other VOCs = 96 TgC yr^{-1}) when forced with the 1850s land cover dataset. Thus, the 1850s–2000s land cover change perturbation reduces the global BVOC emission source strength substantially by ~35%. This value is larger than the 20–25% calculated for pre-industrial to present day in previous studies because it represents the response to the land cover forcing only and does not take into account other global change factors, such as temperature and vegetation productivity, that tend to increase BVOC emissions since the pre-industrial and partially offset the reductions from deforestation. The CH$_4$ chemical lifetime in the 2000s simulation is 10.7 yr, which increases by six months to 11.2 yr in the 2000s simulation forced with 1850s land cover.

The LAND case results in global radiative cooling through O$_3$ (−0.13 W m^{-2}) and CH$_4$ (−0.06 W m^{-2}) and warming through biogenic SOA (+0.09 W m^{-2}), as shown in Fig. 1. The largest single impact of the cropland expansion is through O$_3$. Human deforestation is responsible for substantially lower levels of O$_3$, CH$_4$ and biogenic SOA in the present-day global atmosphere than would exist if the cropland expansion had not occurred. It is well established that, even in the NO$_x$-limited regime, the O$_3$ production efficiency is VOC-dependent. Remarkably, the net atmospheric chemistry effect is a global radiative cooling of −0.11 ± 0.17 W m^{-2}, which is of similar magnitude to the land cover change effects on surface albedo and CO$_2$ compared in Fig. 1.

Conversely, for LAND-fixbvoc, the global-scale effects of the cropland expansion on O$_3$ and biogenic SOA are not statistically

significant relative to interannual variability in the climate model. Instead, there are small but statistically significant global effects on sulphate (+0.01 W m^{-2}), nitrate (−0.01 W m^{-2}) and CH$_4$ (−0.01 W m^{-2}) that give a slight net global cooling of only −0.01 ± 0.02 W m^{-2}, a factor of ten smaller signal than for LAND. The CH$_4$ chemical lifetime decreases by just over a month in the LAND-fixbvoc case. Therefore, I deduce that the global-scale impacts of cropland expansion on the climate pollutants are dominated by the 35% reduction in BVOC emissions and that the non-BVOC mechanisms are not important at the global scale.

The net radiative forcing patterns are spatially inhomogeneous (Fig. 2). The cropland expansion in the LAND case causes widespread reductions in both O$_3$ and biogenic SOA, with especially large effects in the temperate zone, that lead to opposing negative O$_3$ radiative forcing and positive biogenic SOA radiative forcing (Fig. 2). The spatial patterns of the O$_3$ and biogenic SOA perturbations are more spread out than the crop cover increase (Supplementary Fig. 1) because these pollutants have long enough atmospheric lifetimes (a week or more) to undergo long-range intercontinental transport. Furthermore, BVOC oxidation has an intrinsic ability to influence the climate pollutants at large scales far away from the emission source region through the formation of NO$_x$ reservoir species (peroxyacetyl nitrate and alkyl nitrates), which can be transported over vast distances into the free troposphere. The additional cooling effects of the CH$_4$ combine to drive net negative radiative forcing in most regions of the world—except the northern hemisphere transition region between temperate and boreal zones and the tropical savanna region in the sub-Sahara, which exhibit localized positive radiative forcing (Fig. 2). On these regional scales, the biogenic SOA effect outweighs the combined O$_3$ and CH$_4$ effects. Thus, when dark absorbing forest canopies are removed, simultaneous loss of the reflective vegetation aerosol acts to partially compensate the surface albedo increases. Local net negative radiative forcing can exceed −0.3 W m^{-2} and therefore completely offset the land use CO$_2$ forcing at the local scale. The LAND-fixbvoc case has much weaker impacts on net radiative forcing (Fig. 2). In the areas where crop cover increases, a local positive radiative forcing signal is induced. This effect is mostly the result of positive (reduced) reflective sulphate aerosol radiative forcing due to the loss of contrast with the brighter underlying surface albedo when crops replace forests.

This study has newly identified a substantial atmospheric chemistry component due to cropland expansion with a net global cooling radiative impact that is of comparable magnitude to the surface albedo and CO$_2$ radiative effects commonly quantified in climate assessments of human land use. The atmospheric chemistry effects manifest predominantly through altered BVOC emissions. In the conventional paradigm, BVOCs are part of the terrestrial biogeochemical feedback that responds to anthropogenic climate change[18]. This work offers a new perspective: BVOCs as an anthropogenic climate forcing mechanism—instigators of temperature change as well as responses to it. Non-BVOC effects of land cover change have only a minor impact on global atmospheric chemistry but may have much larger local effects in the agricultural areas. The combined atmospheric chemistry and surface albedo global radiative cooling effects from human land cover change may have entirely offset the global radiative warming from the associated CO$_2$ release.

Future reforestation and afforestation strategies, and the potential replacement of native forests with bioenergy plantation forests (strong isoprene emitters), are expected to have the reverse atmospheric chemistry effect on global climate to that of the historical cropland expansion (warming versus cooling). Yet, previous assessments suggest negligible future impacts of atmospheric chemistry–land interactions on global climate due to the compensating influences of physical climate change on
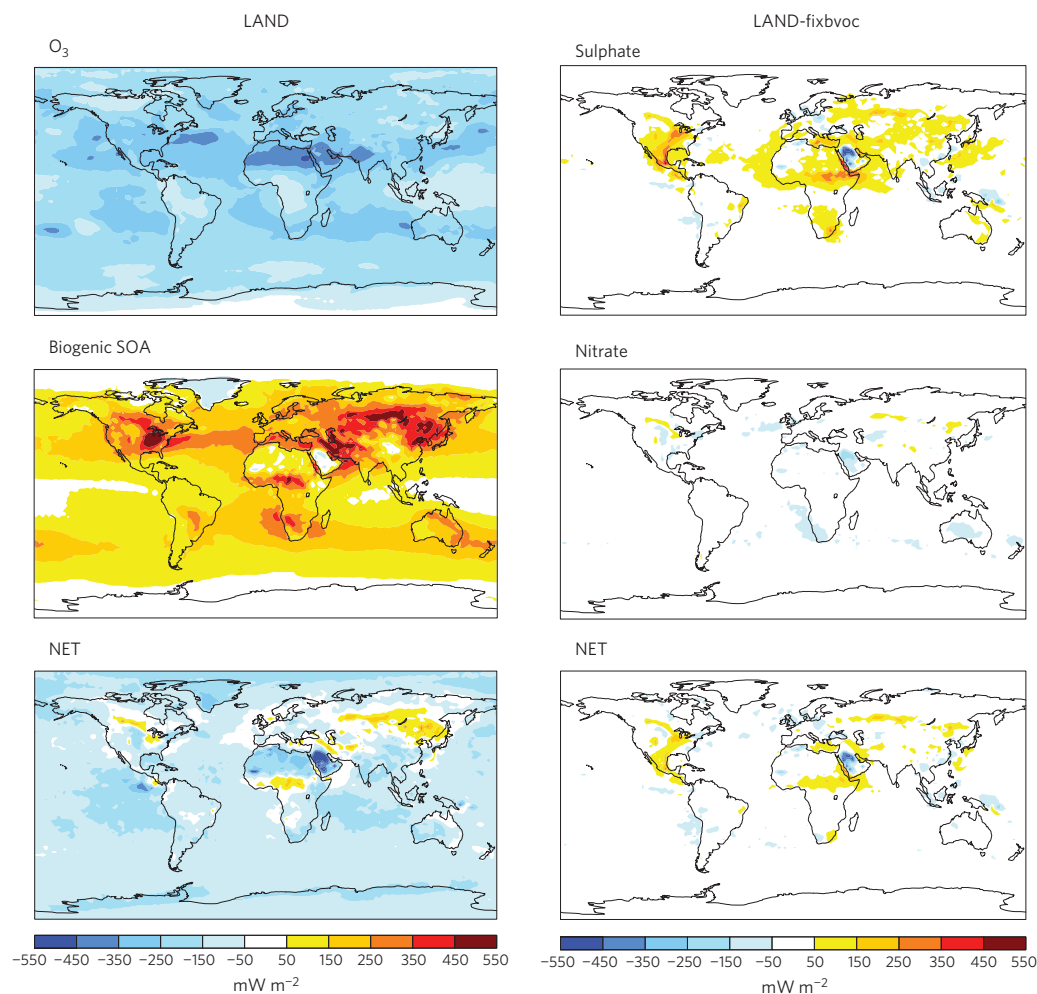
Figure 2 | Spatial distribution of radiative forcing by climate pollutants due to historical cropland expansion (mW m^{-2}). The left column is the LAND case and the right column is the LAND-fixbvoc case. Individual results for the dominant inhomogeneous climate pollutants are shown for each case. The net sum includes the additional homogeneous effects of CH_4.

chemical composition or simply because the global crop cover change in the future scenario is small (∼1.5%; refs 19,20). Future projections of human land use developed for the IPCC AR5 result in global crop cover changes that range from 3–4% increases to 7–9% decreases between 2000 and 2100, less than half the magnitude of the historical change examined in this study[5]. On the basis of these projections, atmospheric chemistry forcing will probably have a smaller impact on global climate in the twenty-first century.

The indirect effect of biogenic SOA on cloud properties and improvements to BVOC oxidation chemistry should be included in the assessment as these processes become better understood. Recent pioneering work has led to important advances in the gas-phase isoprene oxidation mechanism, although uncertainties do still persist[21,22]. Although such improvements in our knowledge of the isoprene oxidation pathways may have significant impacts on simulated local-scale surface O$_3$ and aerosol concentrations, the influence on the global forcing results in this work is likely to be minor. A comprehensive evaluation of human deforestation effects on the climate pollutants would require co-assessment of complex concomitant changes to fire emissions, including fires intentionally set by humans to clear land for agriculture and the loss of wildfire emissions in natural forest ecosystems, and anthropogenic emissions from agricultural land management. Undoubtedly, the sensitivity of the global climate system to BVOC emissions demonstrated here makes a strong case for the establishment of a global-scale long-term monitoring program for BVOC emissions.

Methods

The Yale-E2 global carbon–chemistry–climate model is applied in this study. Yale-E2 is built around the NASA GISS ModelE2 global climate model[23] and includes an interactive land biosphere model[24]. The Yale-E2 framework fully integrates the land biosphere–oxidant–aerosol system so that these components interact with each other and with the physics of the climate model. This study applies 2° × 2.5° latitude by longitude horizontal resolution with 40 vertical layers extending to 0.1 hPa. The atmospheric composition has been well tested against observations[25]. The vegetation submodel is embedded within a general circulation model that provides the key meteorological drivers for the vegetation physiology. The land-surface hydrology submodel provides the grid-cell-level soil characteristics to the vegetation physiology. The vegetation cover is described using eight ecosystem types: tundra, grassland, shrub, savanna, deciduous, tropical rainforest, evergreen and crop. On-line oxidants affect aerosol production and on-line aerosols provide surfaces for chemical reactions and influence photolysis rates. The model includes NO$_x$-dependent biogenic SOA production from the oxidation of BVOC emissions (isoprene, monoterpene and other VOCs; ref. 26) using a two-product scheme that describes partitioning of semi-volatile compounds between the gas and aerosol phases depending on their volatility and pre-existing carbonaceous aerosol availability. O$_3$-initiated isoprene oxidation recycles the hydroxyl radical (OH) but does not represent any additional OH enhancements in forest environments because new evidence suggests that elevated OH field measurements may have been the erroneous result of interference inside the instrument chamber[27]. Alkyl nitrate species that are formed during the oxidation process are 100% available for OH-oxidation to re-release NO$_x$ and peroxy radicals[28].

Leaf isoprene emission is calculated as a function of electron-transport-limited photosynthesis, intercellular and atmospheric CO$_2$ concentration, and canopy temperature[24]. Leaf-level monoterpene emissions are simulated by defining an ecosystem-specific basal rate that is modified using a

temperature-dependent algorithm[29]. Other VOCs emissions are parameterized as 44% of the isoprene emission rate, where 32% of other VOCs are assumed to generate biogenic SOA precursors[26]. The vegetation biophysics module computes the photosynthetic uptake of CO_2 coupled with the transpiration of water vapour and the BVOC emissions at the 30-min physical integration time step of the global model. The global BVOC emission simulation has been extensively evaluated for conditions representative of the present-day climatic state and shown to reproduce 50% of the variance across different ecosystems and seasons in a global database of 28 measured campaign-average fluxes, and to capture authentically the observed variance in the 30-min average diurnal cycle ($R^2 = 64–96\%$) at nine sites where the flux magnitude is simulated to within a factor of two (ref. 24).

The atmosphere-only model simulations apply decadal average (1996–2005) monthly-varying sea surface temperatures and sea ice from the HadSST2 dataset[30]. Anthropogenic emissions of trace gas and aerosol emissions for 2000 are from the historical inventory developed for IPCC AR5 (ref. 13). Long-lived greenhouse gas and CH_4 concentrations are prescribed for the 2000s: $CO_2 = 370$ ppm; $N_2O = 316$ ppb; $CH_4 = 1,752$ ppb; CFC-11 $= 263$ ppt; CFC-12 $= 534$ ppt; other halocarbons $= 363$ ppt. Integrations of 22 model years are completed for all simulations (baseline and sensitivity runs); the first two years of the simulations are discarded as spin-up and the remaining 20 years are averaged for analyses. The simulations include the effects of feedbacks from physical climate change on reactive chemical composition but do not allow the on-line O_3 and aerosol changes to feed back to the radiation and dynamics.

References

1. Myhre, G. *et al.* in *Climate Change 2013: The Physical Science Basis* (eds Stocker, T. F. *et al.*) Ch. 8 (IPCC, Cambridge Univ. Press, 2013).
2. Lathiere, J., Hewitt, C. N. & Beerling, D. J. Sensitivity of isoprene emissions from the terrestrial biosphere to 20th century changes in atmospheric CO_2 concentration, climate, and land use. *Glob. Biogeochem. Cycles* **24**, GB1004 (2010).
3. Pacifico, F., Folberth, G. A., Jones, C. D., Harrison, S. P. & Collins, W. J. Sensitivity of biogenic isoprene emissions to past, present, and future environmental conditions and implications for atmospheric chemistry. *J. Geophys. Res.* **117**, D22302 (2012).
4. Unger, N. Isoprene emission variability through the twentieth century. *J. Geophys. Res.* **118**, 13606–13613 (2013).
5. Hurtt, G. C. *et al.* Harmonization of land-use scenarios for the period 1500–2100: 600 years of global gridded annual land-use transitions, wood harvest, and resulting secondary lands. *Climatic Change* **109**, 117–161 (2011).
6. Brovkin, V. *et al.* Role of land cover changes for atmospheric CO_2 increase and climate change during the last 150 years. *Glob. Change Biol.* **10**, 1253–1266 (2004).
7. Pongratz, J., Reick, C. H., Raddatz, T. & Claussen, M. Biogeophysical versus biogeochemical climate response to historical anthropogenic land cover change. *Geophys. Res. Lett.* **37**, L08702 (2010).
8. Findell, K. L., Shevliakova, E., Milly, P. C. D. & Stouffer, R. J. Modeled impact of anthropogenic land cover change on climate. *J. Clim.* **20**, 3621–3634 (2007).
9. Pitman, A. J. *et al.* Uncertainties in climate responses to past land cover change: First results from the LUCID intercomparison study. *Geophys. Res. Lett.* **36**, L14814 (2009).
10. Guenther, A. B. *et al.* The Model of Emissions of Gases and Aerosols from Nature version 2.1 (MEGAN2.1): An extended and updated framework for modeling biogenic emissions. *Geosci. Model Dev.* **5**, 1471–1492 (2012).
11. Arneth, A. *et al.* From biota to chemistry and climate: Towards a comprehensive description of trace gas exchange between the biosphere and atmosphere. *Biogeosciences* **7**, 121–149 (2010).
12. Shindell, D. T. *et al.* Improved attribution of climate forcing to emissions. *Science* **326**, 716–718 (2009).
13. Lamarque, J. F. *et al.* Historical (1850–2000) gridded anthropogenic and biomass burning emissions of reactive gases and aerosols: Methodology and application. *Atmos. Chem. Phys.* **10**, 7017–7039 (2010).
14. Unger, N. *et al.* Attribution of climate forcing to economic sectors. *Proc. Natl Acad. Sci. USA* **107**, 3382–3387 (2010).
15. O'Donnell, D., Tsigaridis, K. & Feichter, J. Estimating the direct and indirect effects of secondary organic aerosols using ECHAM5-HAM. *Atmos. Chem. Phys.* **11**, 8635–8659 (2011).
16. Scott, C. E. *et al.* The direct and indirect radiative effects of biogenic secondary organic aerosol. *Atmos. Chem. Phys.* **14**, 447–470 (2014).
17. Kiendler-Scharr, A. *et al.* New particle formation in forests inhibited by isoprene emissions. *Nature* **461**, 381–384 (2009).
18. Arneth, A. *et al.* Terrestrial biogeochemical feedbacks in the climate system. *Nature Geosci.* **3**, 525–532 (2010).
19. Ganzeveld, L. *et al.* Impact of future land use and land cover changes on atmospheric chemistry–climate interactions. *J. Geophys. Res.* **115**, D23301 (2010).
20. Ashworth, K., Folberth, G., Hewitt, C. N. & Wild, O. Impacts of near-future cultivation of biofuel feedstocks on atmospheric composition and local air quality. *Atmos. Chem. Phys.* **12**, 919–939 (2012).
21. Paulot, F. *et al.* Unexpected epoxide formation in the gas-phase photooxidation of isoprene. *Science* **325**, 730–733 (2009).
22. Crounse, J. D., Paulot, F., Kjaergaard, H. G. & Wennberg, P. O. Peroxy radical isomerization in the oxidation of isoprene. *Phys. Chem. Chem. Phys.* **13**, 13607–13613 (2011).
23. Schmidt, G. A. *et al.* Configuration and assessment of the GISS ModelE2 contributions to the CMIP5 archive. *J. Adv. Model. Earth Syst.* **6**, 141–184 (2014).
24. Unger, N. *et al.* Photosynthesis-dependent isoprene emission from leaf to planet in a global carbon–chemistry–climate model. *Atmos. Chem. Phys.* **13**, 10243–10269 (2013).
25. Shindell, D. T. *et al.* Interactive ozone and methane chemistry in GISS-E2 historical and future climate simulations. *Atmos. Chem. Phys.* **13**, 2653–2689 (2013).
26. Griffin, R. J., Cocker, D. R., Seinfeld, J. H. & Dabdub, D. Estimate of global atmospheric organic aerosol from oxidation of biogenic hydrocarbons. *Geophys. Res. Lett.* **26**, 2721–2724 (1999).
27. Mao, J. *et al.* Insights into hydroxyl measurements and atmospheric oxidation in a California forest. *Atmos. Chem. Phys.* **12**, 8009–8020 (2012).
28. Mao, J. *et al.* Ozone and organic nitrates over the eastern United States: Sensitivity to isoprene chemistry. *J. Geophys. Res.* **118**, 11256–11268 (2013).
29. Lathiere, J. *et al.* Impact of climate variability and land use changes on global biogenic volatile organic compound emissions. *Atmos. Chem. Phys.* **6**, 2129–2146 (2006).
30. Rayner, N. A. *et al.* Improved analyses of changes and uncertainties in sea surface temperature measured *in situ* since the mid-nineteenth century: The HadSST2 dataset. *J. Clim.* **19**, 446–469 (2006).

Author contributions

N.U. conceived the study, conducted the global model simulations, analysed the model output and wrote the paper.

Additional information

Supplementary information is available in the online version of the paper. Reprints and permissions information is available online at www.nature.com/reprints.

Competing financial interests

The author declares no competing financial interests.